Islamic Azad University

Journal of

Optoelectronical Nanostructures

Volume 10, Issue 3, Autumn 2025, page 45-57

Research Paper (Paper Type)

Optical Density Tuning through Refractive Index Contrast in Periodic and Quasi-Periodic 1D Photonic Crystals

Hadi Rahimi
Department of Physics, Shab.C., Islamic Azad University, Shabestar, Iran

Received: 2024.11.03
Revised: 2025.08.25
Accepted: 2025.08.31
Published: 2025.11.30

Use your device to scan and read the article online

Keywords:
Optical density, Photonic crystals, Refractive Index Contrast, Periodic Structures, Quasi-Periodic Structures

Abstract: This study investigates the optical density (OD) characteristics of one-dimensional photonic crystals (1D PCs) deposited on a polycarbonate substrate, focusing on the comparative performance of periodic and quasi-periodic architectures. Using the transfer matrix method (TMM), four material pairs with varying refractive index contrasts as SiO_2 /ZrO_2 , TiO_2 /MgF_2 , Si/Al_2 O_3 , and Nb_2 O_5 /CYTOP were analyzed under transverse electric (TE) and transverse magnetic (TM) polarizations across a broad spectral range. The results demonstrate that periodic structures exhibit a single, well-defined photonic bandgap, with its width and strength strongly dependent on refractive index contrast, incident angle, and polarization. By contrast, quasi-periodic configurations significantly enrich the spectral response: the Double-Period sequence fragments the broad bandgap into multiple, narrower mini-gaps, while the Thue–Morse arrangement produces an even denser distribution of ultra-narrow resonances. These findings highlight the critical role of structural complexity in tailoring wave attenuation, offering enhanced spectral selectivity, multi-channel filtering, and high sensitivity to angular and polarization variations. Owing to these features, the proposed designs are well-suited for applications in optical filtering, protective coatings, biochemical sensing, and photonic devices requiring tunable light management. Overall, this work establishes the effectiveness of quasi-periodic stacking as a powerful design strategy for engineering next-generation photonic crystal systems.

Citation: Hadi Rahimi. Optical Density Tuning through Refractive Index Contrast in Periodic and Quasi-Periodic 1D Photonic Crystals. **Journal of Optoelectronical Nanostructures**. 2025; 10 (3): 45-57.

***Corresponding author:** H. Rahimi
Address: Department of Physics, Shab.C., Islamic Azad University, Shabestar, Iran.
Email: h_rahimi@iau.ac.ir
DOI: https://doi.org/10.71577/jopn.2025.1189313

1. INTRODUCTION

One-dimensional photonic crystals (1D PCs) have emerged as versatile platforms for manipulating light–matter interactions due to their periodic refractive index modulation along a single spatial direction. Compared to higher-dimensional counterparts, 1D structures offer significant advantages such as design simplicity, ease of fabrication using conventional thin-film deposition techniques, and cost-effective scalability [1]. Their ability to form wide photonic bandgaps enables efficient control of light propagation, while the incorporation of defect layers introduces sharp resonance modes that can be precisely engineered for functional purposes. Owing to these features, 1D PCs have been successfully employed in a wide range of applications, including optical filters, distributed Bragg reflectors, low-threshold lasers, biosensors, light-emitting devices, and energy-harvesting systems [2].

Moving beyond the strictly periodic layers of 1D photonic crystals, quasi-periodic photonic crystals (QPCs) introduce long-range order without translational symmetry, governed by deterministic sequences like Fibonacci or Thue-Morse, which yield intricate band structures with a higher density of resonant states and unique localization properties compared to their periodic analogues [3]. This architectural innovation enables the design of devices with multi-channel, narrowband filtering capabilities, ultra-high quality factor resonators for low-threshold nonlinear optics and enhanced light-matter interaction, and broadband, flat-top reflectors, all while retaining the fabrication-friendly planar geometry of 1D stacks. Furthermore, the inherent self-similarity and richer Fourier spectra of QPCs make them exceptionally promising for applications in optical sensing, where they offer multiple resonance peaks for enhanced sensitivity, and in the development of miniatured, multi-wavelength laser sources and superlenses that leverage their distinctive wave propagation characteristics to overcome the limitations of conventional photonic bandgap materials [4,5].

This unique potential is further diversified by the choice of specific aperiodic sequence, such as Fibonacci [6], Thue-Morse [7], double-period [8], and Rudin-Shapiro [9], each imparting distinct optical characteristics; for instance, Fibonacci sequences excel in generating perfectly self-similar bandgaps ideal for multi-wavelength operation, while Thue-Morse structures exhibit richer Fourier spectra and critical wave localization, enhancing light-matter interaction for lasing and sensing [10]. Double-period sequences offer a compelling compromise, providing a denser hierarchy of photonic bandgaps compared to periodic crystals but with more design flexibility than Fibonacci, and Rudin-Shapiro sequences, being highly disordered, are prized for their broadband, isotropic optical response. Consequently, the selection of a specific quasi-periodic architecture allows for precise tailoring of the photonic density of states, enabling engineers to custom-design devices for applications ranging

from ultra-broadband mirrors and optical computing components to hypersensitive biochemical sensors that exploit the heightened electric field confinement at their many resonant frequencies [11].

The designed photonic crystal structure leverages a selection of complementary dielectric materials to achieve high performance on a polycarbonate substrate. High-refractive-index layers, such as ZrO_2 [12], TiO_2 [13], or Nb_2O_5 [14], provide strong optical confinement and are chosen for their broad transparency, high damage threshold, and compatibility with low-temperature deposition processes. These are paired with low-index materials like SiO_2 [15], MgF_2 [16], or the polymer CYTOP [17] to maximize the refractive index contrast, which is crucial for achieving a wide photonic bandgap. This material selection, deposited via techniques such as sputtering or ALD, ensures excellent mechanical durability, environmental stability, and enables the integration of advanced optical functions onto a flexible, cost-effective platform.

The Beer–Lambert law describes the attenuation of light as it passes through a medium, establishing a logarithmic relationship between transmitted intensity and the product of absorption coefficient, concentration, and path length [18]. This law is widely used to quantify optical density (OD), which serves as a direct measure of light attenuation. In the context of photonic crystals, although light attenuation is primarily governed by multiple reflections and interference rather than material absorption, the Beer–Lambert law provides a useful framework for evaluating OD and comparing the efficiency of different photonic structures. By linking OD to the transmission spectra of one-dimensional photonic crystals, the Beer–Lambert law enables a quantitative analysis of photonic bandgaps, facilitating the design of structures with tailored attenuation in optical filtering, sensing, and light management [19].

The objective of this paper is to systematically compare the optical density responses of three distinct layer configurations: a conventional periodic structure and two quasi-periodic structures based on Double-Period and Thue–Morse sequences. Using four material pairs as SiO_2 /ZrO_2 , TiO_2 /MgF_2 , Si/Al_2O_3 , and Nb_2O_5 /CYTOP on a polycarbonate substrate, the study present spectral analyses to investigate how quasi-periodic arrangements, relative to purely periodic structures, influence and enhance the optical density spectrum. The results can be applied in material spectroscopy, optical sensors, optical window design, light protection systems, and other related fields.

2. THEORY

The optical density (OD) quantifies the light-blocking capability of an optical filter by describing the extent to which the intensity of an incoming beam is reduced. It is directly related to the transmission coefficient (T) and can be expressed as [18, 19]:

$$OD=\log(1/T) \quad (1)$$

Where T represents the transmittance, ranging between 0 and 1. A smaller transmittance value corresponds to a higher OD, meaning stronger attenuation of the incident light. In practice, filters with larger OD values transmit less light and provide stronger absorption, whereas filters with smaller OD values allow higher transmission with minimal attenuation. For instance, an optical density of 2 corresponds to a transmission of only 1%.

Photonic crystals, on the other hand, are artificial periodic structures that strongly affect the propagation of electromagnetic waves. Their optical response is highly dependent on wavelength, giving rise to regions known as photonic bandgaps where light cannot propagate. Depending on the wavelength, photons may either pass through or be reflected by the crystal. To analyze these properties, this study employs the transfer matrix method (TMM), a widely used computational tool for modeling multilayered optical systems [20–25]. For transverse electric polarization, by applying boundary conditions at the interfaces between layers, the transfer matrix between layers is obtained through the following relation:

$$M_j(\Delta z,\omega)=\begin{pmatrix}\cos(k_z^j\Delta z) & j/q_j\sin(k_z^j\Delta z)\\ jq_j\sin(k_z^j\Delta z) & \cos(k_z^j\Delta z)\end{pmatrix} \quad (2)$$

where $k_z^j=(\omega/c)\sqrt{\varepsilon_j}\sqrt{\mu_j}\sqrt{1-\sin^2\theta/\varepsilon_j\mu_j}$ is the wave vector component along the z-axis, ω is the frequency of incident light, c is the speed of light, ε is the dielectric constant of each layer, μ is the magnetic permeability, θ is the angle of incidence, and $q_j=\sqrt{\varepsilon_j}/\sqrt{\mu_j}\sqrt{1-\sin^2\theta/\varepsilon_j\mu_j}$. In this case, the transmission coefficient equals

$$t(\omega,\theta)=\frac{2\cos\theta}{(m_{11}+m_{22})\cos\theta+i(m_{12}\cos^2\theta-m_{21})} \quad (3)$$

Where the coefficients m represent the elements of the transfer matrix for the entire multilayer structure.

3. Results And Discussion

Here, we investigate the optical density of one-dimensional photonic crystals, composed of alternating material pairs (ZrO_2 (A)/SiO_2 (B), TiO_2 (A)/MgF_2 (B), Si(A)/Al_2O_3 (B), and Nb_2O_5 (A)/CYTOP(B)) deposited on a polycarbonate substrate (with a refractive index of 1.59 and thickness of 2 mm), using the Transfer Matrix Method (TMM) implemented in MATLAB software across the visible to infrared wavelength range. The objective is to

systematically compare the optical density responses of three distinct configurations: a conventional periodic structure with period number N=8 and two quasi-periodic structures based on Double-Period and Thue–Morse sequences. The refractive indices and thicknesses of layers A and B are provided in Table 1.

Table 1. Layer Specifications for 1D Photonic Crystal Design

Material Pair	Refractive Index (n)	Δn	Thickness (nm)
ZrO_2 /SiO_2	$n_A=n_{ZrO_2}$ =2.1 $n_B=n_{SiO_2}$ =1.45	0.65	$d_A=d_{ZrO_2}$ =120 $d_B=d_{SiO_2}$ =180
Nb_2 O_5 /CYTOP	$n_A=n_{Nb_2O_5}$=2.2 $n_B=n_{CYTOP}$=1.33	0.87	$d_A=d_{Nb_2\ O_5\ 2}$ =120 $d_B=d_{CYTOP}$=180
TiO_2 /MgF_2	$n_A=n_{TiO_2}$ =2.4 $n_B=n_{MgF_2}$ =1.38	1.02	$d_A=d_{TiO_2}$ =120 $d_B=d_{MgF_2\ 2}$ =180
Si/Al_2 O_3	$n_A=n_{Si}$=3.5 $n_B=n_{Al_2\ O_3}$ =1.76	1.74	$d_A=d_{Si_2}$ =120 $d_B=d_{Al_2\ O_3}$ =180

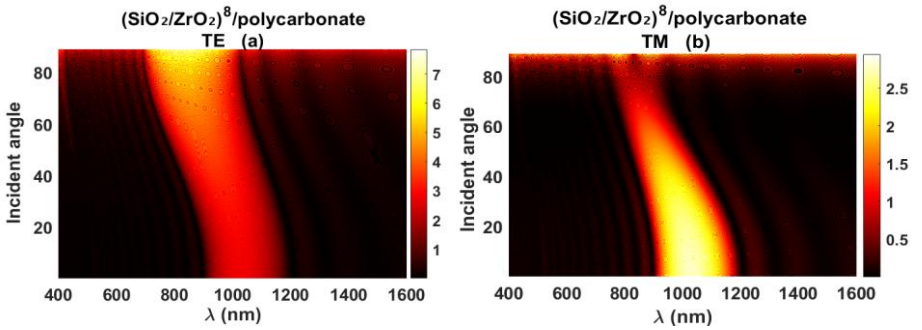

Fig. 1: Optical density of [(SiO_2 /ZrO_2)^8/polycarbonate] for TE (a) and TM (b) polarizations versus wavelength and incident angle

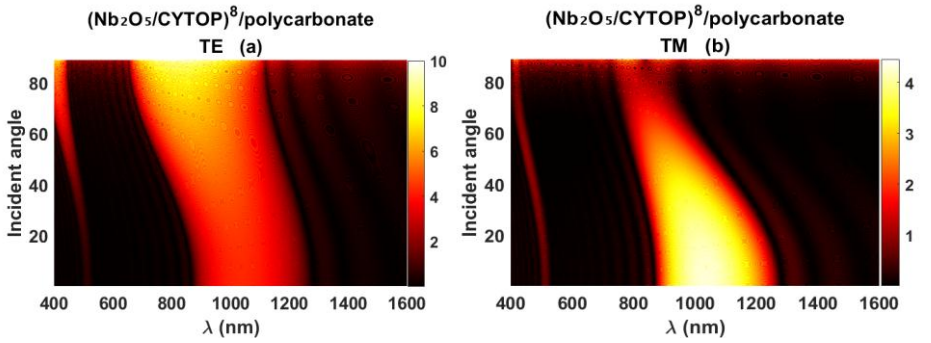

Fig. 2: Optical density of [(Nb_2 O_5 /CYTOP)^8/polycarbonate] for TE (a) and TM (b) polarizations versus wavelength and incident angle

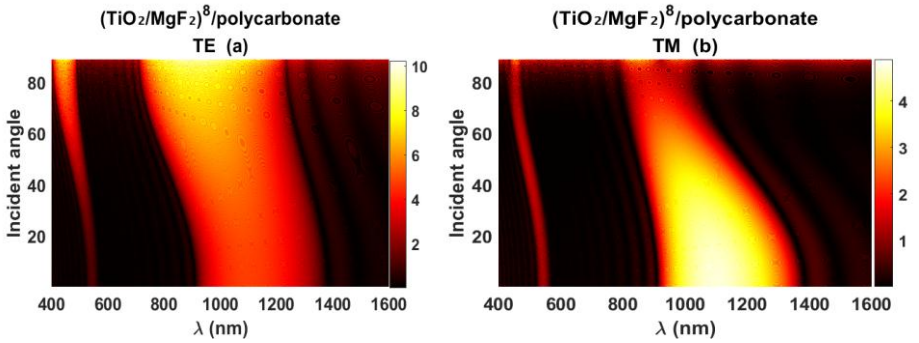

Fig. 3: Optical density of [$(TiO_2/MgF_2)^8$/polycarbonate] for TE (a) and TM (b) polarizations versus wavelength and incident angle

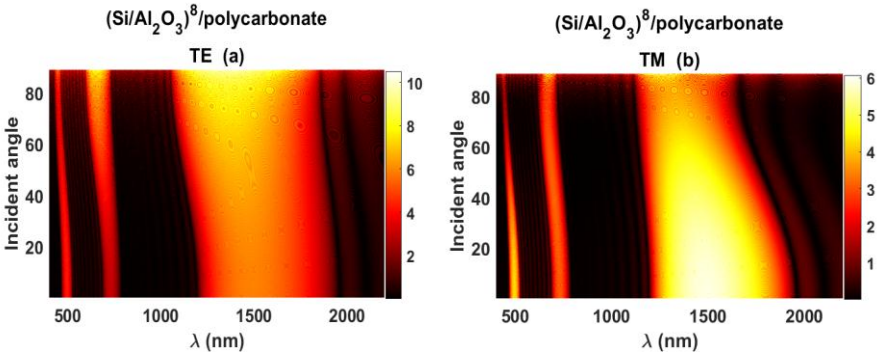

Fig. 4: Optical density of [$(Si/Al_2O_3)^8$/polycarbonate] for TE (a) and TM (b) polarizations versus wavelength and incident angle

Based on the provided optical density plots for the conventional periodic structures with 8 bilayers (Figs. 1-4), several key observations can be made regarding the influence of material composition, incident angle, and polarization. A prominent feature across all figures is the appearance of a photonic band gap (PBG), characterized by a region of high optical density (yellow/red), which indicates strong reflectance and minimal transmission. The central wavelength and width of this band gap are primarily determined by the refractive index contrast between the constituent layers (A and B) and their thicknesses, as per Bragg's law. For instance, the structure with the highest index contrast, Si/Al_2O_3 (Fig. 4), exhibits the broadest and most pronounced band gap, whereas the structure with a lower contrast, such as Nb_2O_5 /CYTOP (Fig. 2), shows a narrower gap. The position of the band gap shifts significantly with the incident angle for both TE and TM polarizations; as the angle increases, the

band gap blueshifts to shorter wavelengths due to the effective change in the optical path length within the layers. Furthermore, the response is highly dependent on the polarization of the incident light. For TM polarization (right panels), the overall optical density, particularly within the band gap region, is generally lower compared to TE polarization (left panels). This is attributed to the Brewster angle effect, which allows TM-polarized light to transmit without reflection at specific angles and wavelengths, thereby reducing the optical density and disrupting the completeness of the band gap. This effect is most visible in structures with higher refractive index layers, such as TiO_2 /MgF_2 (Fig. 3) and Si/Al_2 O_3 (Fig. 4). In conclusion, the results demonstrate that the optical density of a 1D photonic crystal is a strong function of the material's refractive indices, the angle of incidence, and the polarization state of light.

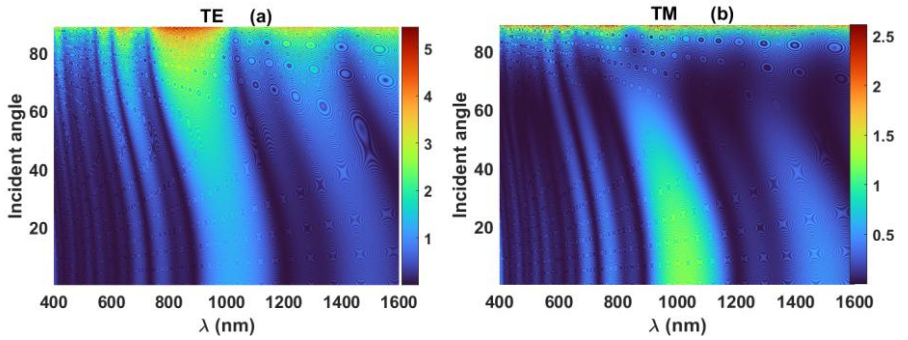

Fig. 5: Same as Fig.1 but for double-period quasiperiodic structure

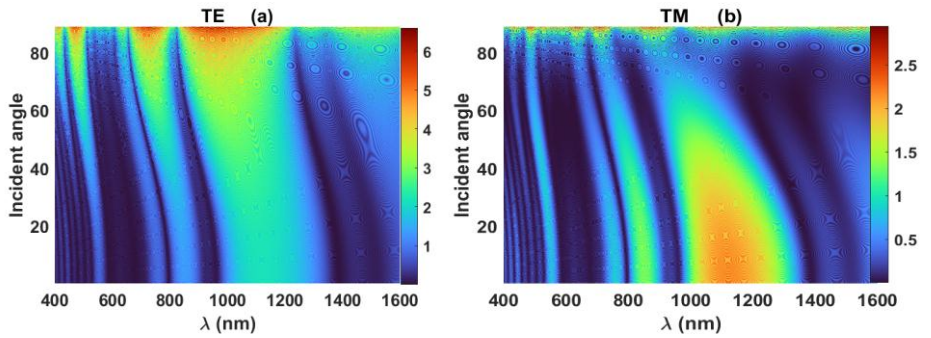

Fig. 6: Same as Fig.2 but for double-period quasiperiodic structure

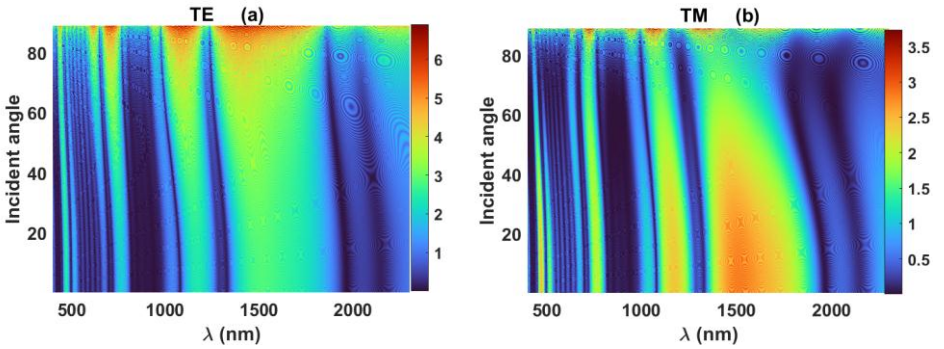

Fig. 7: Same as Fig.3 but for double-period quasiperiodic structure

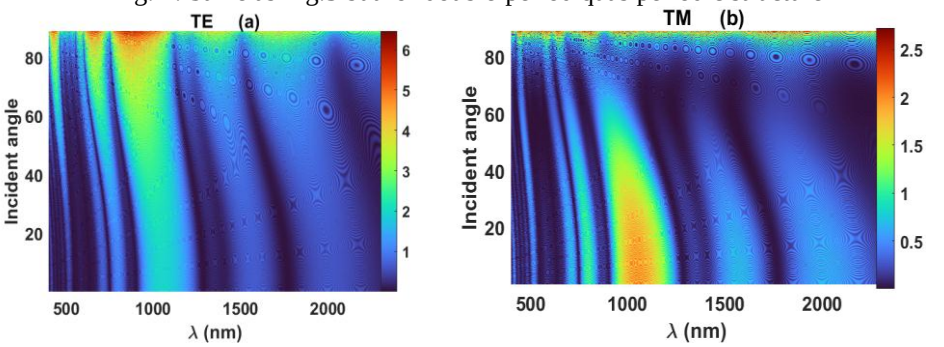

Fig. 8: Same as Fig.4 but for double-period quasiperiodic structure

The optical density plots for the double-period quasiperiodic structures (Figs. 5-8) reveal significant modifications in the photonic response compared to their conventional periodic counterparts (Figs. 1-4). While the fundamental influence of refractive index contrast, incident angle, and polarization remains, the double-period sequence introduces new complexities. The most striking feature is the fragmentation of the primary photonic band gap (PBG) observed in the periodic structures. Instead of a single, continuous region of high optical density, the double-period sequence generates multiple, narrower mini-bandgaps and a higher density of optical states across the spectrum. This is a characteristic outcome of the increased structural complexity and long-range order introduced by the quasiperiodic arrangement, which creates additional Bragg reflection conditions. The contrast in refractive indices remains the primary factor determining the overall strength and visibility of these features; for example, the high-contrast Si/Al_2O_3 structure (Fig. 8) still exhibits the most pronounced and complex pattern of bandgaps, while the lower-contrast Nb_2O_5/CYTOP structure (Fig. 6) shows a more subdued response. The angular and polarization dependence follows the same physical principles but on a more intricate landscape. The blueshift of the various bandgaps with increasing incident angle

is clearly visible for both TE and TM polarizations. However, the TM polarization plots consistently show a reduction in optical density within the bandgap regions compared to TE polarization, similar to the periodic case. This is again due to the Brewster angle effect. The disruption is particularly evident in the high-index structures like TiO_2/MgF_2 (Fig. 7) and Si/Al_2O_3 (Fig. 8), where the defined gaps in the TM mode contrast sharply with the strong, continuous features in the TE mode. In summary, changing the structure from periodic to double-periodic breaks the single, large bandgap into multiple smaller and sharper bandgaps. This creates a more complex optical response, allowing the material to reflect light at several specific wavelengths instead of just one broad range.

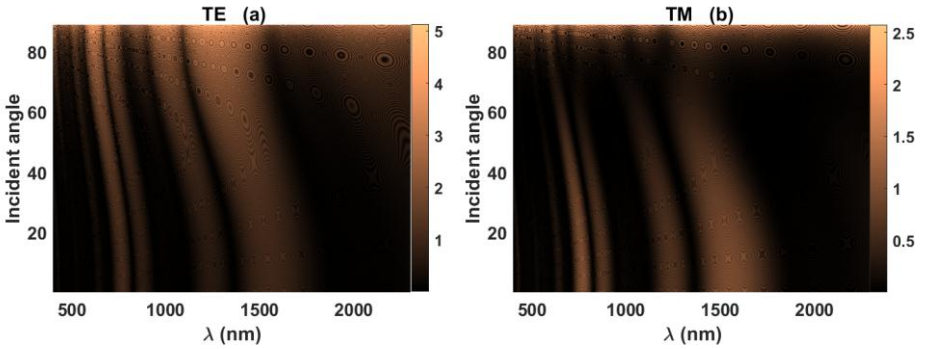

Fig. 9: Same as Fig.1 but for Thue-Morse quasiperiodic structure

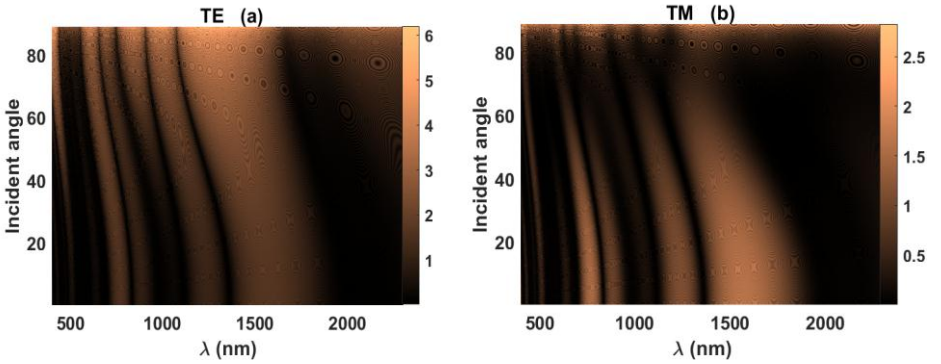

Fig. 10: Same as Fig.2 but for Thue-Morse quasiperiodic structure

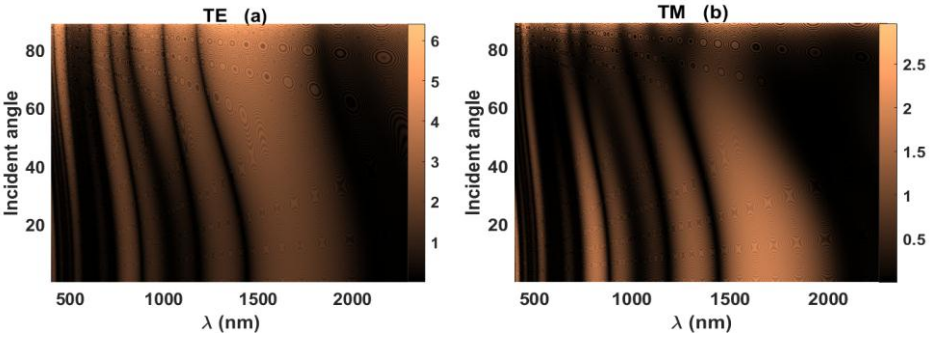

Fig. 11: Same as Fig.3 but for Thue-Morse quasiperiodic structure

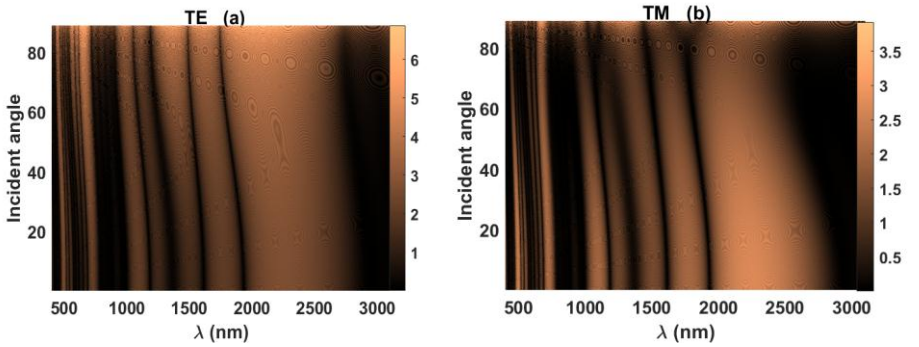

Fig. 12: Same as Fig.4 but for Thue-Morse quasiperiodic structure

The optical density plots for the Thue-Morse quasiperiodic structures (Figs. 9-12) reveal a unique and highly complex photonic response that is distinctly different from both the conventional periodic and double-period structures. The most striking characteristic is the emergence of a highly fragmented and intricate spectrum, featuring a much larger number of very narrow, high-density bandgaps compared to the fewer, broader gaps in the double-period sequence. This creates a much richer and denser optical structure, a hallmark of the Thue-Morse sequence's higher degree of aperiodic order. This extreme spectral complexity makes the Thue-Morse structure highly sensitive to small changes in wavelength, a property ideal for applications like ultra-narrowband filtering and sensing. As with the other structures, the fundamental dependencies remain: the high refractive index contrast pair $Si/Al_2 O_3$ (Fig. 12) produces the strongest and most defined gaps, while the effect is weaker in the low-contrast $Nb_2 O_5$ /CYTOP structure (Fig. 10). Furthermore, the characteristic blueshift of all spectral features with increasing incident angle is clearly observed. The difference between TE and TM polarizations is also pronounced, with the Brewster effect causing a significant reduction in the optical density for TM

polarization, particularly evident within the dense forest of mini-gaps in the high-index structures.

4. CONCLUSIONS

Based on the comprehensive analysis of the optical density, it can be conclusively stated that the transition from a conventional periodic structure to quasi-periodic Double-Period and Thue-Morse sequences fundamentally enhances the photonic response. The key finding is that increasing structural complexity directly translates to greater spectral control: the single, broad photonic band gap of the periodic structure evolves into multiple, sharper mini-gaps in the Double-Period sequence and further fragments into a dense array of ultra-narrowband gaps in the Thue-Morse structure. This progression significantly expands the capability for sophisticated optical filtering and sensing applications. Crucially, these advanced properties remain governed by the fundamental parameters of high refractive index contrast for stronger effects, and are consistently modulated by the incident angle and polarization of light due to the inherent blueshift and Brewster angle phenomena. Therefore, the choice of stacking sequence presents a powerful design degree of freedom for engineering 1D photonic crystals with tailored optical performance.

REFERENCES

[1] V. Ramanathan, K. Muthu, *A review of deep learning based one-dimensional photonic crystals for customizable visible light reflection spectrum*, Journal of Nonlinear Optical Physics & Materials. 15 (2025) 2530001. doi: 10.1142/S0218863525300014.

[2] H. Zhou, D. Li, C. Lee, *Technology Landscape Review of In-Sensor Photonic Intelligence: From Optical Sensors to Smart Devices*. AI Sensors. 1(1) (2025) 5. doi: 10.3390/aisens1010005.

[3] A. Araújo, C. Costa, S. Azevedo, GM. Viswanathan, CG. Bezerra, *Optical properties of 1D photonic time quasicrystals*, Journal of the Optical Society of America B. 42(4) (2025) 949-63. doi:10.1364/JOSAB.542001.

[4] E. Liu, J. Liu, *Quasiperiodic photonic crystal fiber*, Chinese Optics Letters. 21(6) (2023) 060603. doi:10.3788/COL202321.060603

[5] A. Biswal, R. Kumar, H. Behera, IL. Lyubchanskii. *Quasi-periodic one-dimensional photonic crystal as a perspective structures for nanophotonics: analysis of transmittivity spectra*. Materials Science and Engineering: B. 284 (2022) 115915. doi:10.1016/j.mseb.2022.115915.

[6] A. Augustyniak, M. Zdanowicz, T. Osuchm, *Self-similarity properties of complex quasi-periodic Fibonacci and Cantor photonic crystals*. InPhotonics. 8(12) (2021) 558. doi:10.3390/photonics8120558.

[7] J. Wu, Z. Wang, B. Wu, Z. Shi, X. Wu. *The giant enhancement of nonreciprocal radiation in Thue-morse aperiodic structures*. Optics & Laser Technology. 152 (2022) 108138. doi:10.1016/j.optlastec.2022.108138.

[8] F. Segovia-Chaves, H. Vinck-Posada, V. Dhasarathan, *Transmittance spectrum of a double-period photonic structure composed of polymer materials*. Optik. 239 (2021) 166756. doi:10.1016/j.ijleo.2021.166756.
[9] F. Segovia-Chaves, HA. Elsayed. *Transmittance spectrum in a Rudin Shapiro quasiperiodic one-dimensional photonic crystal with superconducting layers*. Physica C: Superconductivity and its Applications. 587 (2021) 1353898. doi:10.1016/j.physc.2021.1353898.
[10] ZA. Zaky, HA. Alqhtani, M. El Malki, I. Antraoui, A. Khettabi, M. Sallah, *Selective filter using Thue–Morse structures by the finite element and transfer matrix methods*. Journal of Computational Electronics. (4): (2025) 120. doi:10.1007/s10825-025-02364-9.
[11] F. Nutku, S. Gökşin, *Comparison of omnidirectional reflectivity of quasi-periodic dielectric multilayers*. Optik. 228 (2021)166220. doi:10.1016/j.ijleo.2020.166220.
[12] M. M. Manziuc, C. Gasparik, M. Negucioiu, M. Constantiniuc. *Optical properties of zirconia: A review of the literature*. EuroBiotech J. 3(1): (2019) 45-51. doi: 10.2478/ebtj-2019-0005.
[13] S. Ge, D. Sang, L. Zou, Y.Yao, C. Zhou, H. Fu, H. Xi, J. Fan, L. Meng, C. Wang. *A review on the progress of optoelectronic devices based on TiO2 thin films and nanomaterials*. Nanomaterials. 13(7): (2023) 1141. doi:10.3390/nano13071141.
[14] C. Nico, T. Monteiro, MP. Graça. *Niobium oxides and niobates physical properties: Review and prospects*. Progress in Materials Science. 80: (2016) 1-37. doi:10.1016/j.pmatsci.2016.02.001.
[15] A. S. Sinitskii, A. V. Knot'ko, Y. D. Tretyakov. *Silica photonic crystals: synthesis and optical properties*. Solid state ionics. 172 (1-4): (2004) 477-9. doi: 10.1016/j.ssi.2004.01.048
[16] CH. Yu, ST. Wicaksono, ST. Wang, TH. Chen. *Electrical and Optical Properties of ZnO: MgF2 with Ag Thin Film for Optoelectronic Sensor Application*. Sensors and Materials. 37(5): (2025) 1825-33. doi:10.18494/SAM5316.
[17] A. Theodosiou, K. Kalli. *Recent trends and advances of fibre Bragg grating sensors in CYTOP polymer optical fibres.* Optical Fiber Technology. 54: (2020) 102079. doi:10.1016/j.yofte.2019.102079.
[18] Mamouei, M., Budidha, K., Baishya, N. et al.: An empirical investigation of deviations from the Beer–Lambert law in optical estimation of lactate. Sci. Rep. 11, 13734 (2021).
[19] Parnis, JM., Oldham, KB.: Beyond the Beer–Lambert law: The dependence of absorbance on time in photochemistry. Journal of Photochemistry and Photobiology A: Chemistry. 267, 6-10 (2013).
[20] L. Missoni, G. Ortiz, M. Martínez-Ricci, V. Toranzos, W. Luis-Mochán. *Rough 1D photonic crystals: a transfer matrix approach*. Opt. Mater. 109 (2020) 110012. doi:10.1016/j.optmat.2020.110012.
[21] A. Karimi, M. Jabbari, G. Solookinejad. *Design and simulation of metal-insulator-metal waveguide for filtering and sensor applications*. *Journal of Optoelectronical Nanostructures*, 8(3) (2023) 90-109. doi:10.30495/jopn.2023.31705.1284.
[22] M. Heidary Orojloo, M. Jabbari, G. Solookinejad, F. Sohrabi. *Design and modeling of photonic crystal Absorber by using Gold and graphene films*. Journal of

Optoelectronical Nanostructures. 7(2) (2022) 1-10. doi: 10.30495/jopn.2022.28915.1235.
[23] M. ZekavatFetrat, M. Sabaeian, G. Solookinejad. *The effect of ambient temperature on the linear and nonlinear optical properties of truncated pyramidal-shaped InAs/GaAs quantum dot*. Journal of Optoelectronical Nanostructures. 6(3) (2021), 81-92. doi: 10.30495/jopn.2021.29138.1240.
[24] Kh. Zarei, G. Solookinejad, M. Jabbari. *Investigating the Properties of an Optical Waveguide Based on Photonic Crystal with Point Defect and Lattice Constant Perturbation*. Journal of Optoelectronical Nanostructures. 1 (1), 2016, 65-80. doi: 20.1001.1.24237361.2016.1.1.6.3
[25] S. M. S. Hashemi Nassab, M. Imanieh, A. Kamaly, *The effect of doping and thickness of the layers on CIGS solar cell efficiency*, J. Optoelectron. Nanostructures. 1(1) (2016) 9-24. doi:20.1001.1.24237361.2016.1.1.2.9.